Novel Optics/Micro-Optics for Miniature Imaging Systems

Jacques Duparré[a] and Reinhard Völkel[b]

[a]Fraunhofer–Institut Angewandte Optik und Feinmechanik, Albert-Einstein-Str. 7, D-07745 Jena, Germany;
[b]SUSS MicroOptics SA, Jaquet-Droz 7, CH-2007 Neuchâtel, Switzerland

ABSTRACT

The visual revolution triggered by the commercial application of digital image capturing devices generates the need for new miniaturized and cheap optical imaging systems and cameras. However, in imaging we can observe only a permanent miniaturization of elements but always similar optical principles are applied which are known to the optical designers for many decades. With the newly gained spectrum of technological capabilities it is the time to ask: Which vision principle should be used at which level of miniaturization and which technology has to be applied in order to achieve the perfectly adapted imaging system? In this paper we present an overview of two insect inspired artificial compound eye concepts for compact vision systems fabricated by lithographic technologies, one classical miniaturized objective and its wafer-scale fabrication and the use of variable focal length liquid lenses for miniaturized autofocus- and zoom objectives without moving parts.

Keywords: Compact vision system, insect vision, artificial compound eye, microlens array, micro–optics

1. INTRODUCTION

Today, the average person is exposed to more than 3,000 visual impressions each day. Our eyes are by far our most powerful information conduit to the brain. We read five times as fast as the average person talks. We register a full-color image, the equivalent of a megabyte of data, in a fraction of a second. When we watch a video, we are seeing about 24 to 30 megabytes of visual information per second. Rich-media mobility is already with us in the form of multimedia laptops, portable projectors, digital cameras, portable storage devices, color-screen PDAs and graphics-enabled handheld computers. PDAs, which had only modest, monochromatic graphical capabilities when they were first introduced, are now being sold with color screens, presentation software and telecom features. Some of the latest cell phones, which were once strictly used for voice communication, have color screens for viewing graphics and even video. Not surprising that this visual revolution generates the need for new miniaturized and cheap imaging systems and cameras.

However, in imaging we only observe a permanent miniaturization of elements but always similar optical principles are applied which are known to the optical designers for many decades. With the newly gained spectrum of technological capabilities it is the time to ask: Which vision principle has to be used at which level of miniaturization and which technology should be applied in order to achieve the perfectly adapted imaging system?! Classical imaging always had its archetype in natural single aperture eyes as, for example, human vision is based on. But not always a high resolution image is required. Often the main aim is on a very compact, robust and cheap vision system.

Natural compound eyes combine small eye volumes with a large field of view, at the cost of comparatively low spatial resolution.[1–3] For small invertebrates as for instance flies or moths the compound eyes are the perfectly adapted solution to obtain sufficient visual information about their environment without overloading their brain with the necessary image processing (Fig. 1). All of theses eye types can use refractive mechanisms for image formation while incorporating graded refractive index optics.[4] In superposition compound eyes, reflective mechanisms can be found as well.[5,6] A natural apposition compound eye consists of an array of microlenses on a curved surface. Each microlens is associated with a small group of photo receptors in its focal plane. Apposition

Further author information: (Send correspondence to Jacques Duparré)
Jacques Duparré: E-mail: jacques.duparre@iof.fraunhofer.de, Telephone: +49 3641 807380
Reinhard Völkel: E-mail: voelkel@suss.ch, Telephone: +41 32 7205103

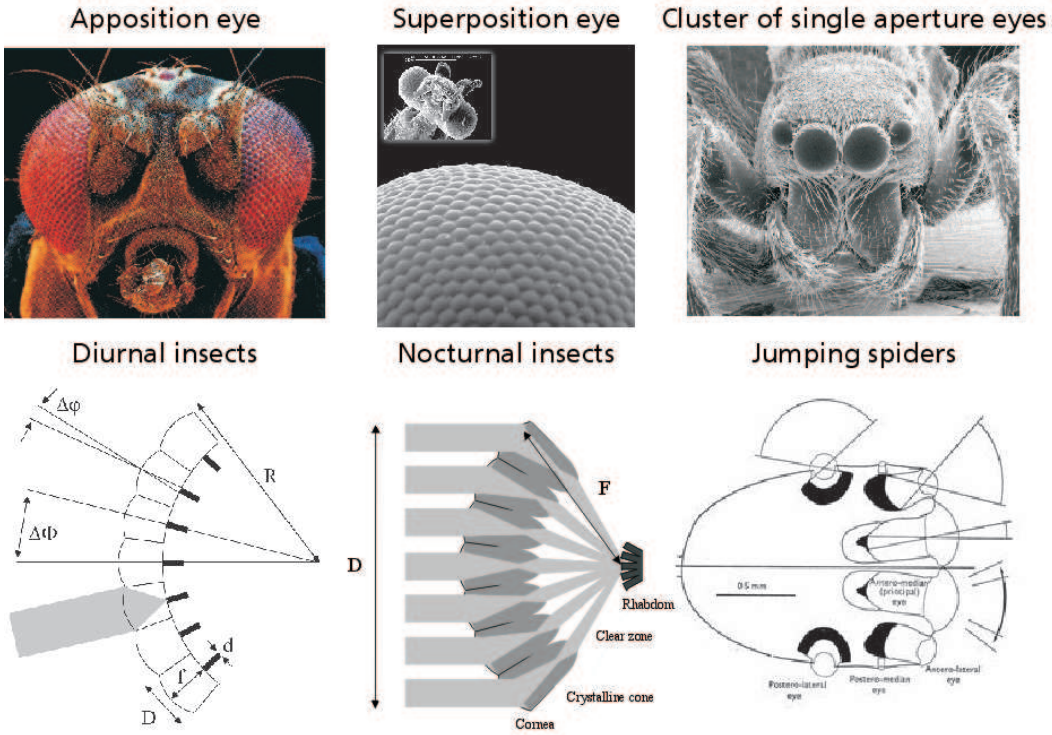

Figure 1. Insect vision. Photographs: "Drosophila melanogaster": Focus Agency; "Ephestia Kuehniella": Institute of applied physics Jena; "Araneae: Salticidae": Aaron Bell; Drawing of jumping spiders head cross section: Wayne & David Maddison)

compound eyes have mainly evolved in diurnal insects such as flies (Fig. 1, left).[7] The single microlens-receptor unit forms one optical channel and is commonly referred to as ommatidium. Pigments form opaque walls between adjacent ommatidia to avoid that light which is focused by one microlens to be received by an adjacent channel's receptor (in case of large angles of incidence). Otherwise ghost images and a reduction of contrast would result. Natural apposition compound eyes contain several hundreds (water fly) up to tens of thousands (honeybee or Japanese dragon fly) of these ommatidia packed in non-uniform hexagonal arrays. The superposition compound eye (Fig. 1, middle) has primarily evolved in nocturnal insects and deep water crustaceans. The light from multiple facets combines on the surface of the photo receptor layer to form a single erect image of the object.[8] For the refractive type, this optical performance is not the result of a single microlens array layer but of an array of microtelescopes. These microtelescopes also incorporate graded index lenses.[9] Compared to natural apposition compound eyes, natural superposition compound eyes are much more light sensitive. In some nocturnal insects, eyes with small $F/\#$, even smaller than one, have been observed. Aberrations – similar to spherical aberrations, but caused by the combination of light combined from many facets – lead to a resolution far from the diffraction limit.[10] In contrast to other insects, jumping spiders have opted for single aperture eyes. But they use eight of them. Jumping spiders possess two high resolution eyes, two wide angle eyes and four additional side eyes (Fig. 1, right). The two antero median eyes provide a magnified image at a high resolution for a rather small visual field.[11] The antero median eyes have a Galilean telescope like optical arrangement[12] leading to a telephoto feature. Jumping spiders use these eyes for detailed inspection of objects of interest. Furthermore, these eyes have a movable retina. This retina can be moved vertically, laterally and rotationally. The spider can track a prey without moving itself. The two antero lateral eyes provide a large visual field at a reduced resolution. The small side eyes cover the large field left and right of the spider. Jumping spiders do not have compound eyes because their resolution would be too poor to identify targets worth to jump to. To be equipped with high resolution single aperture eyes, such as vertebrates, spiders are too small.

Microoptics technology enables the generation of highly precise and uniform microlens arrays with small lens sags and their accurate alignment to the subsequent optics-, spacing- and optoelectronics structures. The result

are thin, simple and monolithic imaging devices with the high accuracy of photo lithography. Artificial compound eyes promise to lead to a completely new class of imaging systems. Due to their compactness artificial compound eyes can find applications, classical objectives will never find their way in. Compound eye cameras should for instance fit into tight spaces in automotive engineering, credit cards, stickers, sheets or displays, security and surveillance, medical technology and shall not be recognized.

Several technical realizations or concepts of imaging optical sensors based on the principle of image transfer through separated channels were presented in the last decade.[13–28] However, since the major challenge for a technical adoption of natural compound eyes consists in the required fabrication and assembly accuracy, most of those attempts have not lead to a breakthrough because usually classical, macroscopic technologies were exploited to manufacture microscopic structures. Sometimes only schematic macroscopic devices were fabricated. It is the aim of this paper to show that these limitations can be overcome by using precise state-of-the-art microoptics technology for the artificial apposition compound eye objective in Section 4 and for the cluster eye in Section 5.

But there is a size of imaging systems where "classical" microoptics technology fails because of the large necessary lens sags. Here, new technologies, combining advantages of classical optical machining and microoptics such as single point diamond turning of lens arrays and wafer-scale replication and stacking of those need to be exploited. This will be introduced next in Section 2 followed by discussion of the optical design using variable focal length liquid lenses for miniaturized autofocus- and zoom objectives without moving parts in Section 3.

2. CLASSICAL MINIATURE OBJECTIVE BY NON-LITHOGRAPHIC WAFERSCALE FABRICATION METHODS

For the low-price fabrication of objectives for the use in mass products like mobile phones or PDAs at present the components of the optics are replicated separately, joined to an objective and are subsequently positioned relative to the imaging electronics (CCD- or CMOS-matrices) individually. This is a high assembly effort, which leads to undesired costs and non-reproducible misalignments and consequently to low yield. Alternatively, our approach uses wafer-scale replication technologies such as hot embossing, which enables a high-precision and cheap production of many equal optical elements parallel on one substrate. But for the large required lens sags, classical microoptics technology such as reflow of photoresist or laser beam writing fails for the master origination. We consequently designed and manufactured a compact three-polymer-lens objective with a minimum of overall length and brilliant optical features where the array-master structures are generated by precision diamond turning. The hot embossed lens plates are subsequently stacked to a sandwich of opto-wafers and a quartz-glass-plate, which carries the dielectric IR cut-off filter on the front side and the CMOS image sensor on the back side, which is connected with the optics-sandwich to build the array of camera-modules at wafer level. We present an objective for a VGA sensor with 640x480 pixels and pixel size of 5.6μm for application in mobile phone cameras, which was designed (patent pending[29]) and experimentally demonstrated by ourselves (Figs. 2 and 3). This objective was specified by the following parameters:

- Length: 4.3mm
- Image circle diameter: 4.5mm
- FOV half angle: 35°
- $F/\#$: 2.8
- MTF: $> 30\%$ at 45LP/mm
- Distortion: $-0.25\% < \Gamma < 0.36\%$

Even though this objective shows an innovative fabrication method, it, on the other hand, demonstrates the limitation of system miniaturization of classical single channel objectives.

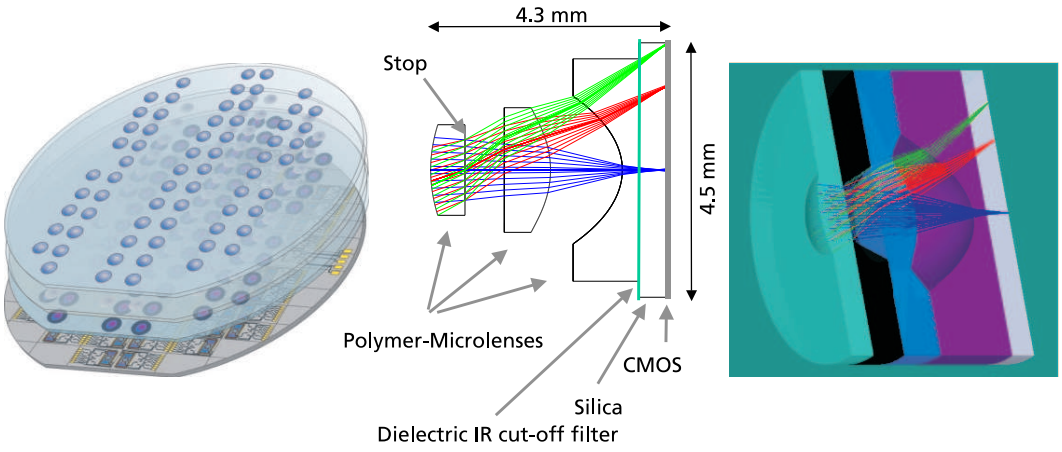

Figure 2. (a) Wafer-scale concept. Optics- and CMOS-wafers are stacked by the use of alignment marks and subsequently the individual camera-modules are separated by dicing. (b) Layout of the designed single aperture objective. (b) Compact triplet incorporating three polymer microlenses and a fused silica plate holding a dielectric IR cut-off filter on the front side. On the substrates backside a thinned CMOS sensor array is located. Between first and second lens a polymer-plate with a conical whole is introduced as system stop and spacing layer. Due to its thickness it also has the function of a field aperture.

Figure 3. (a) Diced polymer-silica-stack building up the objective module. (b) Capture of a radial star pattern filling the objectives FOV. (c) Minimum resolvable feature size of 72LP/mm.

3. MINIATURIZED AUTOFOCUS- AND ZOOM OBJECTIVES BASED ON VARIABLE FOCAL LENGTH LIQUID LENSES

A new principle of variable lenses with tunable focal length has recently been demonstrated by the company Varioptic: Two iso-density non-miscible liquids are trapped inside a transparent cell.[30–32] The liquid-liquid interface forms a drop shape. The natural interfacial tension between liquids produces a smooth optical interface, which curvature is actuated by electrowetting (Fig. 4 (a) and (b)). In addition, in order to have a usable lens, it is necessary to incorporate a centering mechanism, such that optical axis remains stable. Applications of the liquid lenses based on electrowetting can be found in many areas. Typical possible sizes for the lens pupil range from less than a millimeter to one centimeter, using the current technology. This makes this technology ideal for millimetric lenses needed now in the mobile phone applications for autofocus or zoom without mechanically moving parts (Fig. 4 (c)). The very small power consumption (less than one mW dissipated in the lens) is also a great advantage compared to conventional motorized systems. However, optical design studies have shown that there are completely different optical scaling laws for the liquid lens (change of radii of curvature) than for conventional zooms applying mechanically moving lens groups (change of distances). The manufacturing of demonstrations systems is currently underway.

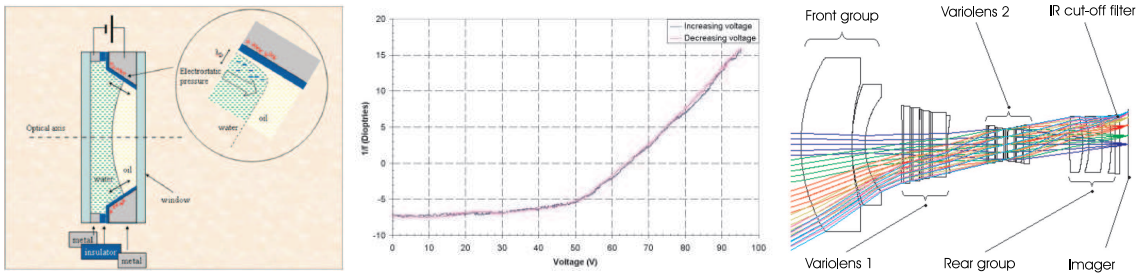

(a) (b) (c)

Figure 4. (a) Schematic drawing of a commercially available liquid lens (Source: VARIOPTIC). (b) Optical power (dioptries) as a function of applied voltage. (c) Schematic drawing of a zoom-objective applying variable focal length liquid lenses.

4. ARTIFICIAL APPOSITION COMPOUND EYE OBJECTIVE

Artificial receptor arrays such as CCD- or CMOS sensors are fabricated on planar wafers. Thus, a thin monolithic objective based on the artificial compound eye concept has to be a planar structure as well. The artificial apposition compound eye consists of a MLA (microlens array) positioned on a substrate, preferably with optical isolation of the channels, and an optoelectronic detector array of different pitch in the microlenses' focal plane.[33] The pitch difference enables different viewing directions of each optical channel. Each channel's optical axis points into a different direction of object space with the optical axes of the channels directed outwards (Fig. 5) if the pitch of the receptor array is smaller than that of the MLA. Consequently, an upright moiré-magnified image results. If the pitch of the MLA is smaller than that of the receptor array, the image is inverted. A pinhole array can be used to narrow the photo sensitive area of the detector pixels if they are not small enough for the required resolution.

A planar artificial apposition compound eye as shown in Fig. 5 is described by the same optical parameters as its curved natural archetype. Behind each microlens a small image of the object is generated. As the result of the pitch difference between MLA and pinhole array, $\Delta p = p_L - p_P$, a moiré-magnified image[34] is obtained when the pinholes with different amounts of offset with respect to the microlenses sample the micro-images.[35] Each channel corresponds to one field angle in object space. The acceptance angle $\Delta\varphi$ determines the trade-off between sensitivity and resolution. It has to be small in order to have a high resolution and large in order to achieve a high sensitivity. The interommatidial angle of the planar apposition compound eye is

$$\Delta\Phi = \arctan\frac{\Delta p}{f}. \tag{1}$$

As in the natural equivalent, opaque walls are introduced between ommatidia preventing cross talk of adjacent channels for object points outside the FOV and resulting ghost images (oblique ray in Fig. 5 (b) demonstrates the ghost effect).

In natural insect eyes the microlens layer as well as the light sensitive cells are both arranged on a curved basis (Fig. 1, left side). Each optical channel focuses the light coming from the object points laying on the channels optical axis. Due to the bending each ommatidium points towards a different angular direction. Therefore these compound eyes exhibit a very large field of view (FOV) while the single channels are working on-axis not suffering from off-axis aberrations.[36] As mentioned above, up to date, artificial apposition compound eye objectives are limited to planar substrates. Consequently the optical channels cannot be arranged in on-axis configurations inherently connected with the appearance of off-axis aberrations when using spherical lenses. In classical macroscopic optical systems, where one optical channel transfers the overall FOV, many optical elements of different refractive indices have to be used in order to minimize off-axis aberrations leading to very complex, bulky and expensive optical systems while they only represent a compromise of aberration correction for all viewing directions.

In contrast, for the apposition compound eye objective each lenslet is assigned only to one angle of the overall FOV. Consequently, an individual correction of the channels for aberrations is feasible.[36] Due to the

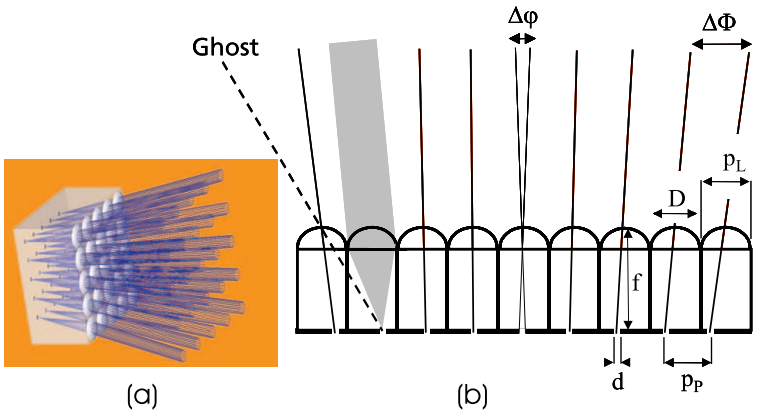

Figure 5. Schematic diagram of a planar artificial apposition compound eye. (a) 3D model of the artificial apposition compound eye showing the focusing MLA, the pinhole array in its focal plane and the tilted optical axes of ommatidia because of a pitch difference between microlens- and pinhole array, enabling the FOV of the imaging system. (b) The thin monolithic device is composed of an array of microlenses with diameter D, focal length f and pitch p_L on the front side of a spacing structure and a pinhole array with pinhole diameters d and pitch p_P in the microlenses' focal plane on the spacing structure's backside.

small numerical aperture of the lenslets of the objective, astigmatism and field curvature are by far dominant compared to coma which is of minor influence. Therefore efficient channel-wise focusing of the oblique angle to be transferred is possible by using different and differently oriented anamorphic lenses for each channel.[37] The radii of curvature of the lenses in the two orthogonal directions (tangential and saggital planes) have to be different and chosen in order to compensate for astigmatism due to the oblique incidence. Furthermore they are both chosen in such a way that the focal plane of all cells with their different angles of incidence is fixed at the position of the paraxial image plane (Fig. 6). This leads to a planarized moiré magnified image[34, 35, 38] in the detector surface. A torus segment having two radii of curvature in perpendicular directions is the most appropriate 3D surface type for such anamorphic lens. A channel-wise decenter of the lens vertex with respect to the assigned receptor center enables for the correction of distortion of the complete objective.

4.1. Fabrication

The fabrication of the artificial apposition compound eye has been carried out using lithographical processes on a wafer scale. It is based on the patterning of a thin 4" glass wafer with arrays of microlenses in a rectangular arrangement on one side and pinhole arrays on the opposite side. The thickness of the wafer is matched to the microlens focal length in the glass.

The generation of the MLAs consists of several steps involving master and mold generation and subsequent UV-replication.[39] The photo resist master pattern is fabricated on a silicon wafer in a standard procedure (photolithography in combination with a heating/reflow process[40]) since it is a well established technology yielding very smooth and well determined spherical surfaces often used for imaging applications.[41] Here the 3D surface is the result of surface tension effects and depends on the volume of the resist cylinder and the shape of the rim of the lens (mask geometry). Consequently stringent limitations to viable geometries apply. A suitable approximation of the desired torus segment is an ellipsoidal lens which can be easily formed by melting a photoresist cylinder on an ellipsoidal basis.[42] For correction of astigmatism and field curvature the ellipses have varying major and minor axes as well as adapted orientations (see Fig. 12, right). The masks of a chirped arrangement, to our knowledge, commercially available mask software tools are not capable to generate. Therefore self-written software tools had to be developed. The required geometry data for the mask necessary for creating the chirped array of ellipsoidal lenses can be derived completely analytically.[43] The replication is carried out in a modified contact mask aligner (SUSS MA6 with UV-embossing option) where the gap between glass wafer and mask/mold is filled by a UV-curing inorganic-organic hybrid polymer which is subsequently cured and separated from the mold. The most critical fabrication issue is the uniformity of the axial distance between microlens vertex and pinhole, affected by a series of parameters like precision of the MA6-height-alignment

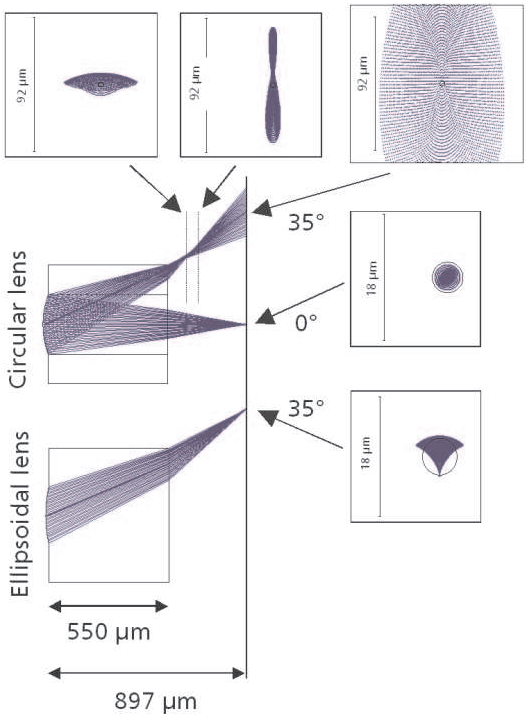

Figure 6. Circular lens and ellipsoidal lens under perpendicular and oblique incidence and related spot diagrams (Arrows indicate the position of the corresponding spot.). A circular lens with radius of curvature R=339μm and diameter D=242.8μm in fused silica (n=1.46 at 550nm wavelength) under perpendicular incidence produces a diffraction limited focus. However, if illuminated under oblique incidence astigmatism and especially field curvature lead to very large spots in the gaussian image plane. The tangential and sagittal image planes are separated from the Gaussian image plane (here -165μm and -262μm, respectively) and the foci are blurred to lines. Using an anamorphic lens with adapted tangential and sagittal radii of curvature (R_t=579μm, R_s=451μm) for this special angle of incidence a diffraction limited spot size is achieved.

($\pm$1μm), bowing of the mold, mask holder, chuck, and substrate ($\pm$6μm overall) as well as by non-uniform microlens focal lengths across the wafer ($\pm$3μm).

An artificial apposition compound eye has a low fill factor of pinholes in the image plane. When combined with a CMOS-imager having a densely packed pixel matrix, the pinhole pitch has to be an integer multiple of the pixel pitch.

The pitch of the artificial apposition compound eyes pinhole array was matched to ten times of the pixel pitch of the sensor array (pixel pitch: 10.6μm). For given FOV of 25° and $F/\#$ of 2.3 a design thickness of 350μm and a MLA pitch of 107.2μm resulted for the objective (Fig. 7). Objective chips with different pinhole sizes covering the photo sensitive area of the sensor pixels were realized on wafer scale in order to examine the influence on resolution and sensitivity (Fig. 8 (a)). The wafers were subsequently diced and the objectives were aligned and glued in front of the detector array[44] within the package (Fig. 8 (b)) and introduced into the PCB (Fig. 8 (c)).

4.2. Experiments

Different test patterns were presented to the artificial compound eye vision system. The captured images are analyzed with respect to resolution and sensitivity, focusing homogeneity and subjective information content. As a result of lacking of opaque walls between the channels in this technological approach, the size of the object presented to the vision system had to be matched to its FOV to avoid cross talk of adjacent channels.

A radial star pattern is well suited to determine the optical cut-off frequency of an imaging system. Here the object frequency is a function of the radial coordinate in the image. The resolution $\chi_{LP/deg}$ in LP/° is estimated

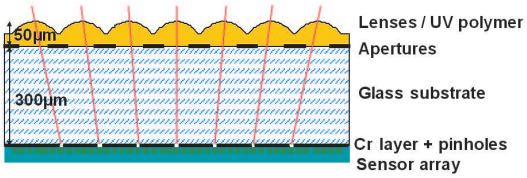

Figure 7. Schematic side view of the fabricated objective, attached to CMOS-sensor array. The MLA layer, replicated into UV-curing polymer, the glass substrate, the metal layer including the pinholes and the optoelectronic sensor array are exhibited.

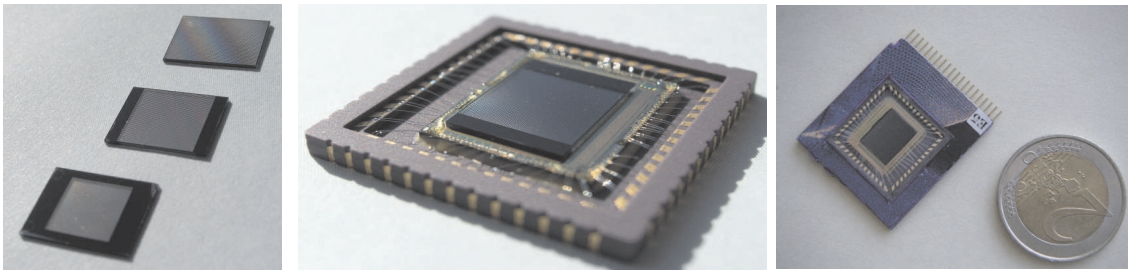

(a) (b) (c)

Figure 8. Diced artificial apposition compound eye objectives. (a) The three fabricated systems: 84x64 channels, 2μm pinhole diameter; 64x64 channels, 3μm pinhole diameter; 50x50 channels, 4μm pinhole diameter. (b) Objective aligned and glued to CMOS-imager in package. (c) Packaged ultra-thin camera. The PCB is of the same thickness as the package. It has an opening where the package is introduced. The whole device is only 1.7mm thin and has a footprint not much larger than a 2 Euro piece (ZMD).

by the cut-off of resolution in the image of the radial star pattern centered within the objective's FOV by

$$\chi_{LP/deg} = \frac{\chi_{LP}}{2\pi\beta}. \tag{2}$$

χ_{LP} is the number of angular LPs in the pattern. β is the angle (unit °) with respect to the optical axis at which the modulation of the angular pattern vanishes.

Figure 9 (a) shows the capturing of a radial star pattern using the artificial apposition compound eye objective. It demonstrates the limitation of resolution by the camera's Nyquist frequency since the cut-off resolution of the device with $d = 2\mu$m pinholes is 1.6LP/° corresponding to 42LPs (corresponding to 84 pixels) over the FOV of 25°.

(a) (b) (c)

Figure 9. Captured test images using an objective with 84x64 channels and 2μm pinhole diameter. (a) Radial star pattern with 18LP filling the FOV. (b) Image of a portrait photograph of Carl Zeiss. (c) Image of "Image Processing Lena".

Figures 9 (b) and (c) show the caption of a portrait photograph of Carl Zeiss and "Image processing Lena", respectively using the artificial apposition compound eye objective. This demonstrates the capability of face recognition.

Bar targets of different spatial frequencies, were imaged for a quantitative MTF determination. Each signal frequency response (SFR) was calculated by a FFT formalism where the amplitude of the first harmonic with respect to the DC peak of the original and the imaged bar patterns are compared and plotted vs. the corresponding angular frequency in Fig. 10. The measured MTF for $d = 2\mu$m pinholes corresponds to the cut-off predicted by the image of the radial star pattern in Fig. 9 (a). Approximately 42LP can be resolved over the entire FOV. The limiting factor of resolution of the generated artificial apposition compound eye objective is the overlapping of the acceptance angles of adjacent channels in object space which increases with increasing pinhole diameters. However, using small pinholes for improvement of resolution results in reduced sensitivity. In Tab.

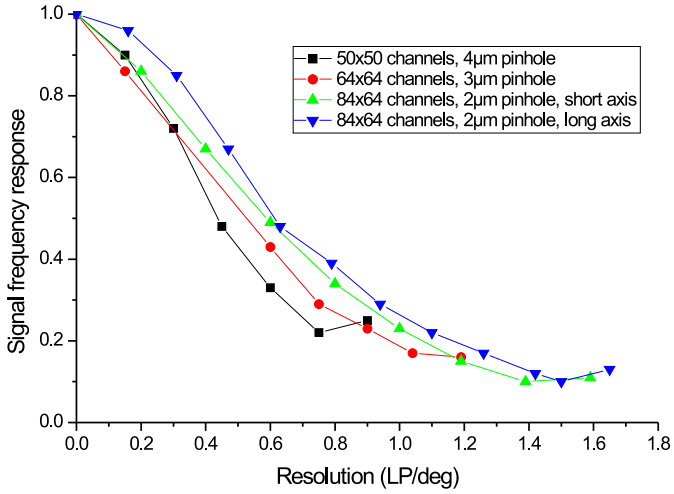

Figure 10. MTF vs. pinhole diameter.

11 the captured optical powers using artificial apposition compound eye objectives with different pinhole sizes are normalized to the power using a bulk objective of the same $F/\#$ and a sensor array with bare pixels for the taking of the same plain image.

Pinhole diameter [μm]	2	3	4
Relative sensitivity [%]	8	17	30

Figure 11. Sensitivity with respect to bulk objective (bare pixel photosensitive area: 7.6x5.3μm^2).

For evaluation of the improved resolution-homogeneity by the use of chirped ellipsoidal microlens arrays we displayed different representative test patterns to a vision system composed of a chirped lens array and for comparison of the regular lens array and investigated the captured images with respect to resolution homogeneity over the FOV. For simplicity only one quadrant of the entire symmetrical FOV is tested, so that the channel in the lower left corner has a perpendicular viewing direction with respect to the objective-plane and consequently applies a circular lens. With increasing viewing angle of the respective channel the ellipticity of the corresponding lens is increased up to an angle of σ_{max}=32° on the diagonal.

Figure 12 shows original bar and radial star test targets, respectively and the corresponding images taken by compound eye objectives applying chirped (cMLA) or regular lens arrays (rMLA). It can be clearly observed that – as to be expected – the resolution in the center of the FOV (lower left corner of objective) is independent of using regular or chirped lens arrays. However, with increasing viewing angle the resolution is decreased when simply using the regular lens array while the resolution stays constant when applying the chirped lens array where each channel is individually optimized for its viewing direction.[45]

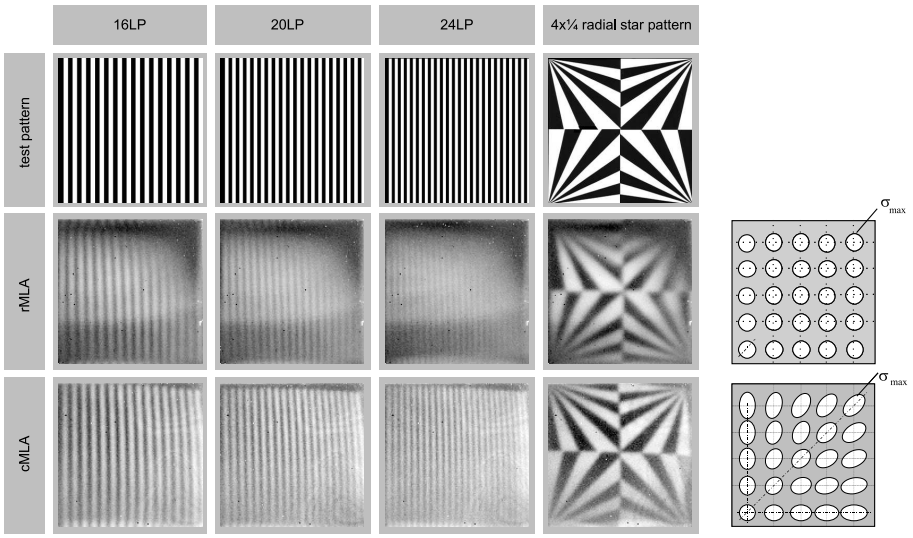

Figure 12. Bar targets of different spatial frequency and captured images of those by using a chirped lens array (cMLA) for channel-wise aberration correction for the oblique incidence and by using a regular lens array for comparison (rMLA). Additionally, a specially adopted 4x1/4 radial star test pattern demonstrates the obtainable resolution in the four image corners as a function of the angle of incidence by the different radii of vanishing contrast of the radial star patterns.

5. CLUSTER EYE

The cluster eye, which is based on a mixture of superposition compound eyes and the vision system of jumping spiders, produces a regular image. Here, three microlens arrays of different pitches form arrays of Keplerian microtelescopes with tilted optical axes, including a field lens- and field aperture array in the intermediate image plane. The arrangement of refracting surfaces is similar to that of a Gabor superlens. The system can be interpreted as a cluster of single pupil microcameras which have tilted optical axes to obtain a large overall FOV. Each channel images only a small angular section. The widths and positions of the field apertures determine the amount of overlap and spatial annexation of the partial-images. The ratio of focal lengths of the telescope lenses and tilt of the optical axes of the telescopes determine the magnification and image annexation.

The parallel transfer of different parts of an overall FOV (different information) with strong demagnification by separated optical channels allows the cluster eye to have a collective space bandwidth product which is equal to the sum of the individual channel's space bandwidth products. Consequently, the cluster eye has the potential of much higher resolution than the experimentally demonstrated artificial apposition compound eye objective. On the other hand the complexity of the cluster eye is much higher as compared with the artificial apposition compound eye objective, and the cluster eye is thicker by a factor of ten. Three wafers of microlens arrays with applied aperture arrays have to be stacked precisely, and there is a high demand on the microlens quality with respect to focal length accuracy. Other advantages of using artificial compound eye imaging systems apply in the same way for the cluster eye as they do for the artificial apposition compound eye objective. Such advantages are the manufacturing of the objective by microoptics technology due to the small required lens sags and correction of each channel for its central viewing direction.

A full description of such a system has to be based on an analytical model to find all reasonable parameter sets and the fundamental relationships. In Ref. 46 it is reported on determination and validation of the first order parameters of a cluster eye in the one-dimensional case using a paraxial 3x3 matrix formalism. The paraxial parameters obtained are transferred to parameters of real microlenses. A 2mm thin imaging system with 21x3 channels, 70°x10° FOV and 4.5x0.5mm^2 image size is optimized using sequential raytracing. Non-sequential raytracing analysis is used for the evaluation of ghost images and stray light of the cluster eye.[47] It is furthermore examined, which sensitivities and resolution can theoretically be obtained. In the following, the fabrication and experimental characterization of tis telescope compound eye imaging system are discussed. The ideal parameters of the finally realized device can be found in Ref. 47.

5.1. Fabrication

A cluster eye with 21x3 optical channels was fabricated by microoptics technology. The microlens shapes are defined by reflow of photo resist cylinders on varying (ellipsoidal) bases. The microlenses are subsequently transferred into fused silica by reactive ion etching. Arrays of apertures with ellipsoidal (focusing array), rectangular (field MLA) and circular openings (relaying MLA) are applied to the corresponding MLAs by chromium etching or lift-off. Finally, the three MLA wafers are stacked in a modified SUSS mask aligner MA8/BA6 with active control of axial distances, wedge error compensation and lateral alignment using appropriate marks. The principle arrangement of the realized cluster eye is given in Fig. 13.

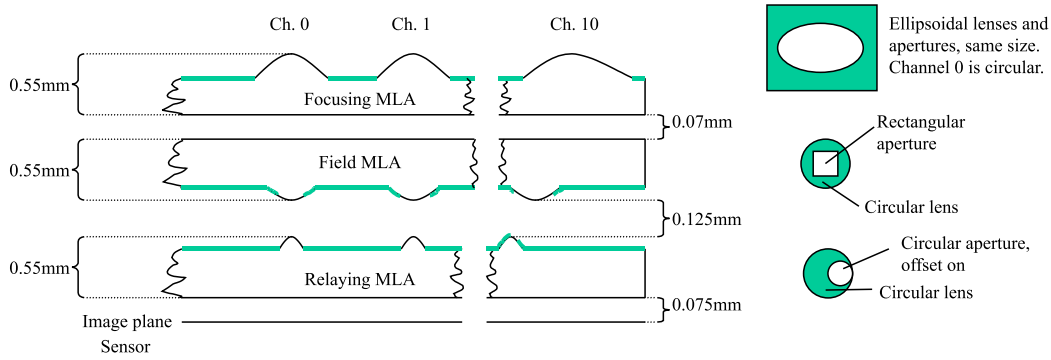

Figure 13. Scheme of experimentally realized cluster eye. The focusing MLA includes ellipsoidal microlenses. The field MLA and the relaying MLA consist of circular microlenses. Chromium apertures are attached to all MLAs. Rectangular field apertures on the field lenses allow a spatial annexation of the partial-images to one regular image. The design total thickness is 1.92mm.

The major issue of the MLA fabrication by reflow process is the predetermination of the microlens shape by the resist height and the shape of the lens-base within the used parameter space.[42] As experiments show, the microlens height is approximately constant for a variation of the resist cylinder base within a certain accuracy,[48] thus the radius of curvature of the microlens is just given by the size of the lens-base.

A critical task in fabrication was to determine the experimentally obtained radii of curvature and deviations of the cross sections of the ellipsoidal lenses from circles in order to find best combinations of fabricated samples of all three layers. Thus, after the RIE-transfer of the photo resist profiles into fused silica the MLAs were characterized by a mechanical stylus instrument which was moved on paths crossing all microlens vertices of the corresponding row or column. Figure 14 demonstrates exemplarily the measured radii of curvature of the focusing array (ellipsoidal microlenses) in comparison to the ideal values. The deviation of the microlens cross sections from a sphere is always below 90nm (RMS). The radius error is below 2%.

The best combination of fabricated MLAs taking into account lens fabrication errors was found by implementing the measured microlens data into the raytracing and optimization software ZEMAX^{TM} and starting a redesign. The degree of freedom left to achieve optimum performance are the axial distances between the arrays defined by the glue thicknesses.

Tolerances for lateral and axial alignment of the different substrates when stacking in the SUSS alignment system are better than $\pm 2\mu$m and $\pm 2.5\mu$m, respectively.

5.2. Experiments

Test patterns were presented to the realized cluster eye and the overall image was relayed onto a conventional CCD camera by a microscope objective with a magnification of x5 and NA=0.18.

The image annexation of all the partial-images can be observed by imaging a white surface, because one smooth white image should be generated. Figure 15 demonstrates that a perfect image stitching could not be obtained with this first demonstrator. Either the partial-images are of roughly rectangular shape but do not connect to each other (Fig. 15 (a)) or they connect only in some portions (Fig. 15 (b)) or have strong overlap in others (Fig. 15 (c)). This causes a considerable intensity modulation even for a smooth white object.

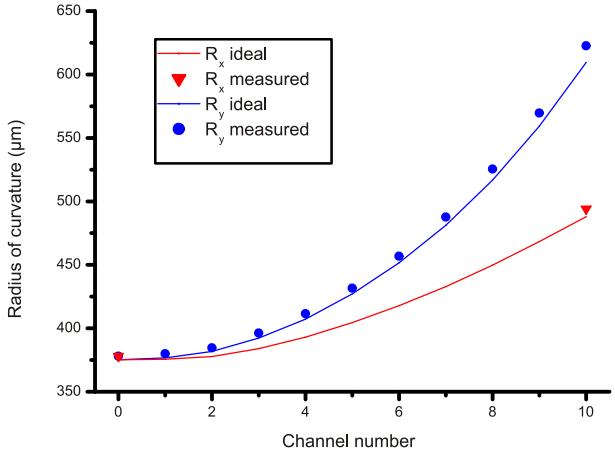

Figure 14. Comparison of ideal and experimentally obtained radii of curvatures of ellipsoidal microlenses of focusing array.

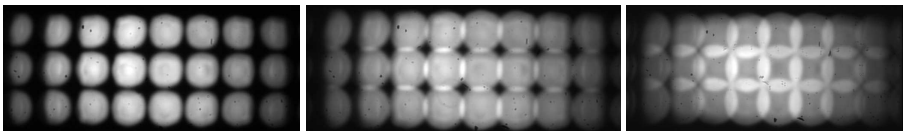

Figure 15. Image of a white surface. (a), (b) and (c) show the same image produced by the cluster eye but with different axial positions of the relay optics (distance of 120μm with respect to each other).

Due the non-telecentric behavior of the cluster eye and the limited NA of the relaying microscope objective, the transmitted field angles are restricted and only a limited number of channels can be observed. However, with the central channels the following images were captured.

Figure 16 shows the images of a radial star pattern, captured at different axial positions from the cluster eye. It can be observed that the matching of the image plane of the individual telescopes with the position of the

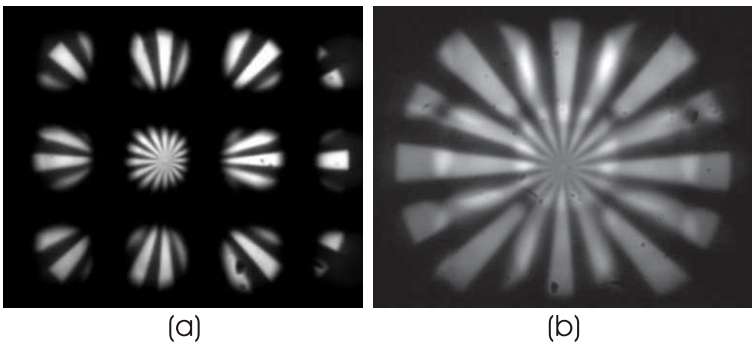

Figure 16. Images of a radial star test pattern at an object distance of 41cm. (Here 5x3 channels are contributing.) (a) At a certain distance from the cluster eye, the partial-images have high contrast but are separated from each other. (b) When moving the image plane 120μm further away from the cluster eye, all the partial-images exhibit a very good annexation with only minor areas of overlap or lack of annexation. One regular image is generated by transfer of the different image section through separate channels. However, the contrast of the partial-images is reduced compared to (a) because the image plane of the telescopes is slightly defocused.

perfect annexation of the partial-images is particularly critical. This is mainly influenced by the correspondence of the axial position of the intermediate images with the position of the field apertures. The poor quality of the produced field apertures is considered to be less important. Tolerances of MLA fabrication and assembly are very tight (in the μm order of magnitude) and there are no compensation possibilities without reducing

either contrast of the partial-images or degrading the image stitching. However, it is demonstrated that one overall image is generated by the transfer of the different image section through separated channels with a strong demagnification. Each channel has a FOV of 4.1°x4.1°, the size of the partial-images is 192x192μm^2. This results in a magnification with an equivalent focal length of 2.75mm at a system length of the realized cluster eye of only 1.99mm equivalent to a telephoto ratio of 1.4. Images of bar targets of different spatial frequencies were taken to quantitatively determine the cluster eyes resolution to 3.3LP/°.

6. CONCLUSIONS AND OUTLOOK

The technically achieved resolutions of 1.6LP/° of the artificial apposition compound eye objective and 3.3LP/° for the cluster eye seem rather promising compared to today's standard imaging devices, if the difference in system length of approximately one order of magnitude is taken into account. For comparison: A classical single aperture wide-angle objective with 70° horizontal field of view and a 1 Megapixel sensor provides an angular resolution of 7.1LP/° if homogeneous resolution over the field of view is assumed. The total track of such a "miniature" single aperture objective is typically in the order of magnitude of 5-10mm. The angular resolution of the demonstrated artificial compound eyes is furthermore comparable to that of many invertebrate eyes such as e.g. the honey bee (0.5LP/°) or the jumping spider (3-6LP/°). The natural archetypes show: It is not the highest resolution that provides the optical solution capable of surviving for millions of years, but the simplest solution in perfect adaptation to the image capturing task and to the environmental circumstances such as minimum volume, no need for focusing for different object distances, and minimum necessary signal processing.

Finally, comparing the analyzed artificial compound eye concepts with their natural archetypes the following conclusions can be drawn: The major difference at this stage of development is the planar arrangement of the artificial systems compared to the curved geometry of the natural ones. This is the consequence of today's limitation to planar lithographic patterning technologies. However, artificial compound eye imaging systems, besides compactness and large telephoto ratio, exhibit one major advantage for solving the problem of off-axis aberrations: Because of the segmented image transfer each channel can be specially optimized for its individual viewing direction resulting in a drastically improved resolution homogeneity over the objectives entire FOV while classical single-channel-imaging-systems always have to be a compromise for all the angles of incidence represented in the FOV.

ACKNOWLEDGMENTS

The work presented in Section 2 (classical miniature objective by non-lithographic waferscale fabrication methods) was funded by the European Commission within the project "WAfer Level Optic solution foR compact CMOS Imager." (IST-2001-35366: WALORI). The work presented in Section 4 (artificial apposition compound eye objective) is funded by the German Federal Ministry of Education and Research (BMBF) within the project "Extrem flache Kamerasysteme für Anwendungen im Automobil" (X-FLAKSA, FKZ: 13N8796). We would like to acknowledge the contributions of A. Bräuer, P. Schreiber, P. Dannberg and their technical staff from the Fraunhofer Institute of Applied Optics and Precision Engineering (IOF), Jena. P. Dannberg is responsible for the fabrication of the different types of artificial apposition compound eye objectives using microoptics technology. His exceptionally good aligned UV-replication of microlens arrays is the key of the successful fabrication of the presented demonstrators. F. Wippermann (IOF) we would like to appreciate for the design of the chirped ellipsoidal lens arrays. He is also working on the optical design using variable focal length liquid lenses for zoom and auto-focus applications. The waferscale replication of classical objectives for mobile phone applications took place in the company "Fresnel Optics" in Apolda, Germany (M. Bitzer and S. Schreiter). The experience of M. Eisner (from SUSS MicroOptics SA (Neuchâtel, Switzerland) in aligned stacking of microlens array wafers finally lead to the realization of the waferscale VGA-objectives and the cluster eye. We are furthermore very thankful for the help we got from our colleagues from the Institute of Microtechnology (IMT) of the University of Neuchâtel, Switzerland, especially T. Scharf who took very important steps in the fabrication of the lens- and aperture arrays of the cluster eye. We would also like to acknowledge J. Werner and W. Mierau from the "Zentrum Mikroelektronik AG Dresden" (ZMD), Germany, and M. Goede and M. Verhoeven from "Aspect Systems", Dresden, Germany, for the distribution of the CMOS sensor array and its readout periphery, respectively, which we combined with the artificial apposition compound eye objectives to a digital camera.

REFERENCES

1. J. S. Sanders, ed., *Selected Papers on Natural and Artificial Compound Eye Sensors*, SPIE Milestone Series, SPIE Optical Engineering Press, Bellingham, 122 ed., 1996.
2. M. F. Land and D.-E. Nilsson, *Animal Eyes*, Oxford Animal Biology Series, Oxford University Press, Oxford, 2002.
3. A. W. Snyder, D. G. Stavenga, and S. B. Laughlin, "Spatial Information Capacity of Compound Eyes," *J. Comp. Physiol. A* **116**, pp. 183–207, 1977.
4. S. Exner, *Die Physiologie der facettierten Augen von Krebsen und Insecten*, Deuticke, Leipzig, 1891.
5. M. F. Land, "Animal eyes with mirror optics," in *Sci. Am.*, 6, ed., 126-134, (December), 1978 239.
6. M. F. Land, "Eyes with mirror optics," *Pure Appl. Opt.* **2**, pp. R44–R50, August 2000.
7. K. G. Goetz, "Die optischen Uebertragungseigenschaften der Komplexaugen von Drosophila," *Kybernetik* **2**, pp. 215–221, 1965.
8. M. F. Land, "The optics of animal eyes," *Contemp. Phys.* **29**, pp. 435–455, September/October 1988.
9. P. McIntyre and S. Caveney, "Graded index optics are matched to optical geometry in the superposition eyes of scarab beetles," *Phil. Trans. R. Soc. Lond. B* **311**, pp. 237–269, 1985.
10. M. F. Land, F. Burton, and V. Meyer-Rochow, "The Optical Geometry of Euphausiid Eyes," *J. Comp. Physiol. A* **130**(1), pp. 49–62, 1979.
11. M. F. Land, "Structure of the retinae of the principal eyes of jumping spiders (salticidae: dendryphantinae) in relation to visual optics," *J. exp. Biol.* **51**, pp. 443–470, 1969.
12. D. S. Williams and P. McIntyre, "The principal eyes of a jumping spider have a telephoto component," *Nature* **288**, pp. 578–580, 1980.
13. J. S. Sanders and C. E. Halford, "Design and analysis of apposition compound eye optical sensors," *Opt. Eng.* **34**, pp. 222–235, January 1995.
14. K. Hamanaka and H. Koshi, "An artificial compound eye using a microlens array and its application to scale-invariant processing," *Opt. Rev.* **3**(4), pp. 264–268, 1996.
15. S. Ogata, J. Ishida, and T. Sasano, "Optical sensor array in an artificial compound eye," *Opt. Eng.* **33**, pp. 3649–3655, November 1994.
16. F. Mura, I. Shimoyama, and K. Hoshino, "A One–chip Scanning Retina with an Integrated Micromechanical Scanning Actuator," *J. of Microelectromech. Syst.* **10**(4), pp. 492–497, 2001.
17. N. Franceschini, J. M. Pichon, and C. Blanes, "From insect vision to robot vision," *Phil. Trans. R. Soc. Lond. B* **337**, pp. 283–294, 1992.
18. Y. Kitamura, R. Shogenji, K. Yamada, S. Miyatake, M. Miyamoto, T. Morimoto, Y. Masaki, N. Kondou, D. Miyazaki, J. Tanida, and Y. Ichioka, "Reconstruction of a high–resolution image on a compound–eye image–capturing system," *Appl. Opt.* **43**, pp. 1719–1727, March 2004.
19. D. Gabor, "Improvements in or relating to optical systems composed of lenticules," *Pat.* UK 541,753, December 1940.
20. M. Hutley, R. F. Stevens, and C. Hembd, "Imaging Properties of the "Gabor Superlens"," in *Digest of Top. Meet. on Microlens Arrays at NPL, Teddington*, M. C. Hutley, ed., **EOS 13**, pp. 101–104, 1997.
21. M. C. Hutley, "Integral photography, superlenses and the moiré magnifier," in *Digest of Top. Meet. on Microlens Arrays at NPL, Teddington*, M. C. Hutley, ed., **EOS 2**, pp. 72–75, 1993.
22. M. Kawazu and Y. Ogura, "Application of gradient-index fiber arrays to copying machines," *Appl. Opt.* **19**, pp. 1105–1112, April 1980.
23. W. B. Hugle, R. Daendliker, and H. P. Herzig, "Lens array photolithography," *Pat.* US 8,114,732, 1993.
24. R. H. Anderson, "Close-up imaging of documents and displays with lens arrays," *Appl. Opt.* **18**, pp. 477–484, February 1979.
25. V. Shaoulov and J. P. Rolland, "Design and assessment of microlenslet–array relay optics," *Appl. Opt.* **42**, pp. 6838–6845, December 2003.
26. P. Nussbaum, R. Völkel, H. P. Herzig, M. Eisner, and S. Haselbeck, "Design, fabrication and testing of microlens arrays for sensors and Microsystems," *Pure Appl. Opt.* **6**, pp. 617–636, 1997.

27. R. Völkel, M. Eisner, and K. J. Weible, "Miniaturized imaging systems," *Microelectron. Eng.* **67-68**, pp. 461–472, 2003.
28. R. Völkel, "Natural optical design concepts for highly miniaturized camera systems," in *Design and Eng. Optical Syst. II*, **3737**, pp. 548–556, SPIE, August 1999.
29. J. Duparré, P. Schreiber, P. Dannberg, A. Bräuer, and M. Bitzer, "Miniaturisiertes Objektiv für digitale Kameras und Herstellung im Wafer-Maßstab," *Pat.* DE 10 2004 036 469.9, 2004.
30. B. Berge and J. Peseux, "Variable focal lens controlled by an external voltage: an application of electrowetting," *Eur. Phys. J. E* **3**, pp. 159–163, 2000.
31. C. Gabay, B. Berge, G. Dovillaire, and S. Bucourt, "Dynamic study of a varioptic variable focal lens," in *Proc. of Current Developments an Lens Design and Optical Engineering III*, R. E. Fischer, W. J. Smith, and R. B. Johnson, eds., **SPIE 4767**, pp. 159–165, 2002.
32. L. Saurei, J. Peseux, F. Laune, and B. Berge, "Tunable liquid lens based on electrowetting technology: principle, properties and applications," in *Proc. of 10th Microopt. Conf.*, W. Karthe, G. D. Khoe, and Y. Kokubun, eds., **ISBN: 3-8274-1603-5**, pp. E–1, Elsevier, 2004.
33. J. Duparré, P. Dannberg, P. Schreiber, A. Bräuer, and A. Tünnermann, "Artificial apposition compound eye fabricated by micro–optics technology," *Appl. Opt.* **43**, pp. 4303–4310, August 2004.
34. R. F. Stevens, "Optical inspection of periodic structures using lens arrays and moiré magnification," *Imaging Sci. J.* **47**, pp. 173–179, 1999.
35. H. Kamal, R. Völkel, and J. Alda, "Properties of moiré magnifiers," *Opt. Eng.* **37**, pp. 3007–3014, November 1998.
36. T. Hessler, M. Rossi, J. Pedersen, M. T. Gale, M. Wegner, and H. J. Tiziani, "Microlens arrays with spatial variation of the optical functions," in *Digest of Top. Meet. on Microlens Arrays at NPL, Teddington*, M. C. Hutley, ed., **EOS 13**, pp. 42–47, 1997.
37. S. Sinzinger and J. Jahns, "Integrated micro–optical imaging system with a high interconnection capacity fabricated in planar optics," *Appl. Opt.* **36**, pp. 4729–4735, July 1997.
38. M. C. Hutley, R. Hunt, R. F. Stevens, and P. Savander, "The moiré magnifier," *Pure Appl. Opt.* **3**, pp. 133–142, 1994.
39. P. Dannberg, G. Mann, L. Wagner, and A. Bräuer, "Polymer UV-molding for micro-optical systems and O/E- integration," in *Proc. of Micromachining for Micro–Optics*, S. H. Lee and E. G. Johnson, eds., **SPIE 4179**, pp. 137–145, 2000.
40. Z. D. Popovich, R. A. Sprague, and G. A. N. Conell, "Technique for monolithic fabrication of microlens arrays," *Appl. Opt.* **27**(7), pp. 1281–1284, 1988.
41. R. Völkel, H. P. Herzig, P. Nussbaum, and R. Dändliker, "Microlens array imaging system for photolithography," *Opt. Eng.* **35**(11), pp. 3323–3330, 1996.
42. N. Lindlein, S. Haselbeck, and J. Schwider, "Simplified Theory for Ellipsoidal Melted Microlenses," in *Digest of Top. Meet. on Microlens Arrays at NPL, Teddington*, M. C. Hutley, ed., *EOS* **5**, pp. 7–10, 1995.
43. F. Wippermann, J. Duparré, P. Schreiber, and P. Dannberg, "Design and fabrication of a chirped array of refractive ellipsoidal micro-lenses for an apposition eye camera objective," in *Proc. of Optical Design and Engineering II*, L. Mazuray and R. Wartmann, eds., *SPIE* **5962**, pp. 59622C–1 – 59622C–11, 2005.
44. J. Duparré, P. Dannberg, P. Schreiber, A. Bräuer, and A. Tünnermann, "Thin compound eye camera," *Appl. Opt.* **44**, pp. 2949–2956, May 2005.
45. J. Duparré, F. Wippermann, P. Dannberg, and A. Reimann, "Chirped arrays of refractive ellipsoidal microlenses for aberration correction under oblique incidence," *Opt. Exp.* **13**, pp. 10539–10551, December 2005.
46. J. Duparré, P. Schreiber, and R. Völkel, "Theoretical analysis of an artificial superposition compound eye for application in ultra flat digital image acquisition devices," in *Proc. of Optical Design and Engineering*, L. Mazurany, P. J. Rogers, and R. Wartmann, eds., *SPIE* **5249**, pp. 408–418, 2003.
47. J. Duparré, P. Schreiber, A. Matthes, E. Pshenay-Severin, A. Bräuer, A. Tünnermann, R. Völkel, M. Eisner, and T. Scharf, "Microoptical telescope compound eye," *Opt. Exp.* **13**, pp. 889–903, February 2005.
48. J. Duparré, P. Schreiber, P. Dannberg, T. Scharf, P. Pelli, R. Völkel, H.-P. Herzig, and A. Bräuer, "Artificial compound eyes–different concepts and their application to ultra flat image acquisition sensors," in *Proc. of MOEMS and Miniaturized Systems IV*, A. El-Fatatry, ed., *SPIE* **5346**, pp. 89–100, 2004.